

Multilevel Nonlinear Mixed-Effects Models for the Modeling of Earlywood and Latewood Microfibril Angle

Lewis Jordan, Richard F. Daniels, Alexander Clark III, and Rechun He

Abstract: Earlywood and latewood microfibril angle (MFA) was determined at 1-millimeter intervals from disks at 1.4 meters, then at 3-meter intervals to a height of 13.7 meters, from 18 loblolly pine (*Pinus taeda* L.) trees grown in southeastern Texas. A modified three-parameter logistic function with mixed effects is used for modeling earlywood and latewood MFA. By making the parameters of the logistic function linear functions of height, a three-dimensional model was developed that describes the changes of earlywood and latewood MFA within the tree. A first-order autoregressive correlation structure and a variance model corresponding to a variance covariate given by the fitted values for each wood type, but in which the proportionality constant differs according to the level of wood type, was identified as the within-group correlation and variance structures. Cross-validation was used to determine model accuracy and precision. The methods of model development including determination of the height structure, which parameters should be considered random or fixed, determination of an appropriate variance-covariance structure, and prediction are addressed. Model performance was evaluated utilizing informative statistics including likelihood ratio tests (LRTs), Akaike information criterion (AIC), and Bayesian information criterion (BIC). FOR. SCI. 51(4):357–371.

Key Words: Microfibril angle, mixed effects models, nonlinear models, loblolly pine, repeated measurements.

L OBLLOLY PINE (*PINUS TAEDA* L.) is the most important commercial species in the southern United States. The southeastern states produce 58 and 16% of all the marketed timber in the United States and the world, respectively (Wear and Greis 2002). Loblolly pine is used extensively for use in the manufacture of lumber and composite wood products, and is the primary species of the US pulp and paper industry (Daniels et al. 2002). Microfibril angle (MFA) is known to be one of the main determinants of the mechanical properties of wood. MFA is defined by Lichtenegger et al. (1999) as the angle between the cellulose fibrils and the longitudinal cell axis. MFA is highly correlated with specific gravity, modulus of elasticity, modulus of rupture, and the longitudinal and tangential shrinkage of wood. MFA has a significant effect on both the mechanical behavior and dimensional stability of wood, and as such is an important quality characteristic for sawn timber (MacDonald and Hubert 2002). In addition, MFA has been correlated with differences in paper properties such as stretch, stiffness, and strength (Watson and Dadswell 1964, Kellogg et al. 1975, Megraw 1985). Because of these relationships, MFA has become an important indicator of wood quality to the forest products industry.

Variations in MFA of any tree species can be attributed to variation within a tree, between trees in a particular stand, between different growing sites, and between different sil-

vicultural regimes (Addis et al. 1995). MFA varies within each growth ring, from pith to bark, with height in the stem and among trees. Cave and Walker (1994) reported that the MFA decreases from the first earlywood cell to the last latewood cell. MFA in loblolly pine is large near the pith and decreases rapidly out to 10 or more rings from the pith, and then continues dropping, regardless of height, but at a much slower rate until such time as it essentially stabilizes. The decrease in MFA with age takes place at a slower rate near the base of the tree than it does in the upper region. This results in higher MFA values for a given number of rings from the pith at the butt and breast height regions than at several meters in height and above (Megraw 1985). Megraw et al. (1999) found that the average MFA values of 24 loblolly pine trees decreases with increasing ring number all the way out through ring 20 at the base, 1 meter, and 2 meters in height. At heights of 3 meters and above, MFA was found to decrease to ring 10, where it essentially stabilized near 10° for all rings thereafter.

MFA varies considerably within the juvenile and mature zones of tree wood. MFA is characteristically greater in juvenile wood than mature wood. In juvenile wood MFA is large, ranging from 25° to 35° and often up to 50° near the pith, while MFA in mature wood is small, ranging from 5° to 10° (Larson et al. 2001). Pillow et al. (1953) found that MFA in the juvenile wood of open-grown loblolly pine

Lewis Jordan, Research Coordinator, Warnell School of Forest Resources, The University of Georgia, Athens, GA 30602-2152—Phone: (706) 542-9724; Fax: (706) 542-0119; lcj6444@forestry.uga.edu. Richard F. Daniels, Professor, Warnell School of Forest Resources, The University of Georgia, Athens, GA 30602-2152—Phone: (706) 542-7268; ddaniels@forestry.uga.edu. Alexander Clark III, Wood Scientist, USDA Forest Service, Southern Research Station, Athens, GA 30602—Phone: (706) 559-4323; aclark@fs.fed.us. Rechun He, Graduate Research Assistant, Warnell School of Forest Resources, The University of Georgia, Athens, GA 30602-2152—Phone: (706) 542-9724; rxh0951@forestry.uga.edu.

Acknowledgments: The authors gratefully acknowledge support from the sponsors of the Wood Quality Consortium of the University of Georgia, Boise-Cascade, Georgia-Pacific, International Paper, MeadWestvaco, Plum Creek, Smurfit-Stone, Temple-Inland, Weyerhaeuser, and the USDA Forest Service. We also thank the editor, associate editor, and the three anonymous reviewers at Forest Science for their helpful and insightful comments.

Manuscript received August 25, 2004, accepted February 22, 2005

Copyright © 2005 by the Society of American Foresters

averaged 20° larger than that of closely spaced natural stands. MFA has been found to decrease from 33° at ring 1 to 23° by age 10, and 17° at age 22, in fast-grown loblolly pine (Ying et al. 1994).

Nonlinear mixed-effects models (NLMEs) are important tools for statistical modeling with forestry applications. Recently, Fang and Bailey (2001) used NLMEs for modeling dominant height growth curves of slash pine (*Pinus elliottii* Engelm.) under varying silvicultural scenarios. Hall and Clutter (2004) describe techniques for development of multivariate multilevel NLMEs for prediction of dominant height, basal area, trees per hectare, and volume. Daniels et al. (2002) used a three-parameter logistic function for modeling specific gravity of loblolly pine at any ring from pith and height.

Forestry-related data are typically collected from permanent plots over time, e.g., height, basal area, volume, and trees per hectare. The assumption of independence of repeated measures in forestry is often violated by the repeated sampling of permanent plots, or in our case individual trees (Clutter 1961, Bailey and Clutter 1974, Lappi and Bailey 1988, Gregoire et al. 1995). Data of this structure accommodate analysis using mixed-effects modeling techniques. NLMEs allow for the inclusion of multiple sources of correlation and/or heterogeneity, and account for treatment or covariate effects with fixed-effects parameters (Hall and Clutter 2004).

In this article we use repeated measures at the individual tree and disk level for development of multilevel nonlinear mixed-effects models for modeling earlywood and latewood MFA in three-dimensional space. We also present the methods of model development including determination of the height structure, determination of random and fixed parameters, determination of an appropriate variance-covariance structure, and prediction.

Study Materials

Eighteen trees representing six stands were selected from southeastern Texas for MFA analysis. The stands were located on land owned by forest products companies, and included only stands with similar silvicultural history: (1) site preparation with no herbaceous weed control, (2) no fertilization at planting except phosphorus on phosphorus-deficient sites, and (3) stand density of at least 617 trees per hectare at the time of sampling. Trees larger than 12.7 centimeters in diameter were inventoried on three 0.04-hectare plots to determine stand density and diameter distribution. A sample of three trees proportional to the diameter distribution of each stand to represent a range of tree sizes in the stand was chosen for MFA analysis. Stand attributes are summarized in Table 1.

Cross-sectional disks 2.54 centimeters thick were cut at 1.4 meters, and then at 3-meter intervals to a height of 13.7 meters. A radial strip 1.27 centimeters square in cross-section, extending from pith to bark, was cut from each disk, dried, glued to core holders, and sawn into two strips at the pith. The strip used for MFA analysis was dried at 122°C

Table 1. Range and average tree size (in parenthesis) characteristics for 18 loblolly pine trees sampled for earlywood and latewood MFA analysis in Southeast Texas.

DBH (cm)	Total Height (m)	Age (years)	Earlywood MFA (degrees)	Latewood MFA (degrees)
14.2–29.0 (20.0)	11.4–21.7 (17.2)	21–24 (22)	8.2–39.8 (17.9)	8.1–33.7 (15.1)

and analyzed by Silviscan using X-ray diffraction at 1-millimeter intervals on the radial surface. A densitometer was used to determine specific gravity. The densitometer was calibrated to express specific gravity on an air-dried basis and a specific gravity value of 0.53 was used to separate earlywood and latewood. Traditionally, a specific gravity value of 0.48 is used to distinguish between earlywood and latewood specific gravity (Clark et al. 2004) based on green volume and dry weight. However, specific gravity values analyzed by Silviscan are based on dry volume and dry weight resulting in a reduction of volume on the order of 10%, thus resulting in higher specific gravity values. Separation of earlywood rings from latewood rings was accomplished using Silviscan's Analyse2001 program. A plot of mean annual ring MFA by wood type and disk height is presented in Figure 1. It can be seen that the both earlywood and latewood follow the same general pattern. At all heights, MFA is large near the pith and decreases rapidly until it eventually stabilizes. Figure 1 also indicates that MFA is larger in earlywood than latewood at all height levels.

Model Development

A modified three-parameter logistic function serves as the basic MFA model. The model can be expressed as

$$f(\text{Ring}) = \frac{\beta_0}{1 + e^{\beta_1 \text{Ring}}} + \beta_2, \quad (1)$$

where Ring is ring number from pith, $f(\text{Ring})$ is the mean

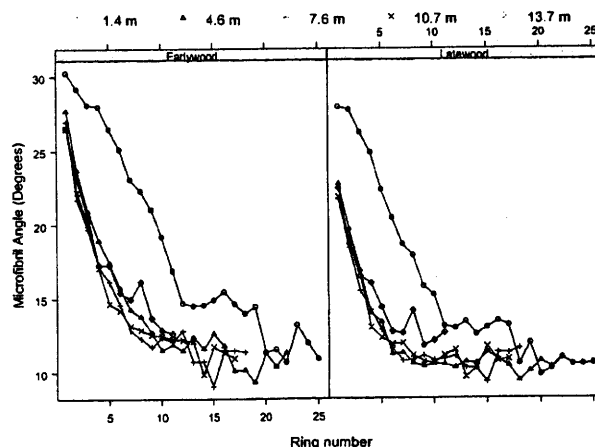


Figure 1. Plot of mean microfibril angle by wood type and height level (m).

response function of MFA, β_0 corresponds to an initial value parameter, β_1 is the rate parameter, and β_2 is the lower asymptote. If β_1 is positive, as $\text{Ring} \rightarrow \infty$, $f(\text{Ring}) \rightarrow \beta_2$. To represent MFA in three-dimensional space, height must be added as a covariate. In this case, the parameters β_0 , β_1 , and β_2 were allowed to vary with height. That is, the parameters are to be taken as functions of height. By allowing the parameters in Equation 1 to be both fixed and random effects, the obtained random effects estimates can be plotted by height, indicating an appropriate function, i.e., linear, quadratic, or some higher-ordered polynomial function.

Using the notation of Pinheiro and Bates (2000), let y_{ijk} equal the response at the k th measurement on the j th second-level group of the i th first-level group. This can be expressed as

$$y_{ijk} = f(\beta_{ijk}, v_{ijk}) + \varepsilon_{ijk} \quad (2)$$

$$i = 1, \dots, M, \quad j = 1, \dots, M_i, \quad k = 1, \dots, n_{ij},$$

where M is the number of first-level groups (trees), M_i is the number of second-level groups within the i th first-level group (disks within a tree), n_{ij} is the number of observations on the j th second-level group of the i th first-level group, and ε_{ijk} is a normally distributed within-group error term. Here, f is a real-valued, differentiable function of vector-valued mixed-effects parameters β_{ijk} and a vector of covariates v_{ijk} . The mixed-effects parameters β_{ijk} take the form

$$\beta_{ijk} = A_{ijk}\beta + B_{ijk,1}b_i + B_{ijk,2}b_{ij}, \quad (3)$$

where b_i and b_{ij} are the first- and second-level random effects vectors of size $q_1 \times 1$ and $q_2 \times 1$, respectively. $B_{ijk,1}$ and $B_{ijk,2}$ are the associated random effects design matrices, respectively. The fixed effects design matrix and parameter

vectors are A_{ijk} and β , respectively. We assume $b_i \sim N(0, \Psi_1)$, $b_{ij} \sim N(0, \Psi_2)$. No constraints other than assuming they are positive-definite symmetric matrices are put on Ψ_1 and Ψ_2 . It may be useful to restrict Ψ_1 and Ψ_2 to special forms of variance-covariance matrices for stability and computing speed. By assuming the random effects are independent of each other, it would make Ψ_1 and Ψ_2 diagonal matrices. Hall and Clutter (2004) state that often there is no a priori reason for assuming the random effects parameters are uncorrelated, and that random effects pertaining to distinct response variables measured on the same unit will typically be correlated. The models in this article were fit using the NLME library in S-Plus.

Specification of the Height Structure

For development of an appropriate height structure, independent random effects were assumed implying a diagonal random effects variance-covariance matrix with zero off-diagonal covariance elements. After determination of the height structure, the assumption of independent random effects will be relaxed, and a correlated variance-covariance structure will be applied to account for potential correlation among the random effects. All models fit in this study used the natural logarithm of disk height. Taking the natural logarithm of disk height rescales the slope of the height structure, paying dividends in computational time and model stability. Plots of the random effects estimates by parameter versus the natural logarithm of height are given in Figure 2. From the plot, it appears that β_0 is linearly correlated with the natural logarithm of height, β_1 is quadratic, and β_2 possibly linearly correlated with the natural logarithm of height. The fitting comparison of differing height structures (Table 2) indicates that the assumptions

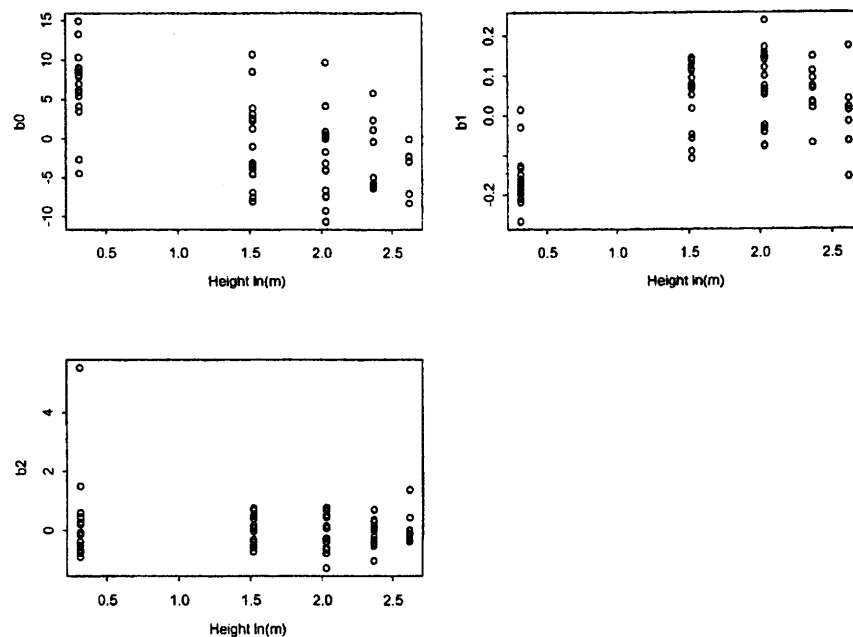


Figure 2. Plot of estimated random effects versus the natural logarithm of height (m).

made above are plausible (model 3). Because the models are nested, a likelihood ratio test (LRT) can be used to determine which model contains the appropriate height function. LRTs show that the model where all parameters are quadratic functions of height (model 1) can be reduced to a more parsimonious model. Table 2 also indicates that a height term is needed in the β_2 parameter (model 5).

From Table 2, model 3 will be used to represent three-dimensional earlywood and latewood MFA based on LRT, log-likelihood, AIC and BIC criteria, and parsimony. Because the basic model structure has been specified, it may now be appropriate to relax the assumption of independence among the random effects estimates. We first update model 3 by fitting a general positive-definite variance-covariance structure. We also test whether the second-level random effects (disks within tree) can be eliminated from the model using LRTs. Table 3 indicates that a correlated variance-covariance structure is needed in the model. The LRT comparing the diagonal and symmetric variance-covariance structures was found to be almost significant at the 0.001 level. Furthermore, the LRT statistic confirms the significance of the second-level random effects (disks within tree).

Adding Earlywood and Latewood Covariates into the Model

We are now interested in determining which covariates in the data are potentially useful in explaining random effects variation. In this case, we are interested in explaining the relationship/variation of earlywood and latewood MFA. High correlation of the random effects may be an indicator that similar patterns exist among the design components, which may be explained by some other covariates (Fang and Bailey 2001). A plot of the random effects shows the correlations among the three random effects parameters are high (Figure 3), indicating a covariate model for the mixed effects may be helpful in explaining variation. One way for determining the relationship between the mixed effects and the covariates (earlywood and latewood) is to plot the random effects estimates against these covariates. However, the measurements of earlywood and latewood are dependent because they were taken from the same ring within the same disk. This restricts us in plotting the estimated random

effects by wood type, but these covariates may still be included in the model by adding indicator variables. Updating model 4 from Table 3, the new model, call it model 4.1, takes the form

$$MFA_{ijk} = \frac{\beta_{0ij}}{1 + e^{\beta_{1ij}Ring}} + \beta_{2ij}$$

$$\beta_{ij} = \begin{pmatrix} \beta_{0ij} \\ \beta_{1ij} \\ \beta_{2ij} \end{pmatrix} = \begin{pmatrix} \beta_0 \\ \beta_1 \\ \beta_2 \end{pmatrix} + \begin{pmatrix} b_{0i} \\ b_{1i} \\ b_{2i} \end{pmatrix} + \begin{pmatrix} b_{0ij} \\ b_{1ij} \\ b_{2ij} \end{pmatrix}$$

$$= \begin{pmatrix} (\beta_{00} + \beta_{01}I_x + b_{0i} + b_{0ij}) + (\beta_{02} + \beta_{03}I_x)\ln(ht) \\ (\beta_{10} + \beta_{11}I_x + b_{1i} + b_{1ij}) + (\beta_{12} + \beta_{13}I_x)\ln(ht) \\ \quad + (\beta_{14} + \beta_{15}I_x)\{\ln(ht)\}^2 \\ (\beta_{20} + \beta_{21}I_x + b_{2i} + b_{2ij}) + (\beta_{22} + \beta_{23}I_x)\ln(ht) \end{pmatrix}, \quad (4)$$

$$I_x = \begin{cases} 1, & \text{if wood type} = \text{Latewood} \\ 0, & \text{if otherwise.} \end{cases}$$

The addition of the covariates in the model may change the variance-covariance correlation of the estimated random effects at both the tree and disk levels. This suggests that some of the random effects may be dropped, or the variance-covariance structure could be simplified by assuming some block diagonal structure. Updating model 4.1, call it model 4.2, we allow

$$\text{Var}(b_i) = \text{Var} \begin{pmatrix} b_{0i} \\ b_{1i} \\ b_{2i} \end{pmatrix} = \Psi_1 = \begin{pmatrix} 0 & 0 & 0 \\ 0 & \psi_{11} & \psi_{12} \\ 0 & \psi_{21} & \psi_{22} \end{pmatrix},$$

and

$$\text{Var}(b_{ij}) = \text{Var} \begin{pmatrix} b_{0ij} \\ b_{1ij} \\ b_{2ij} \end{pmatrix} = \Psi_2 = \begin{pmatrix} \psi_{00} & 0 & \psi_{02} \\ 0 & \psi_{11} & 0 \\ \psi_{20} & 0 & \psi_{22} \end{pmatrix}.$$

In Ψ_1 (the tree level), we removed the b_{0i} random effects parameter, which was found to be significantly smaller than the b_{1i} and b_{2i} random effects estimates, and assume an unstructured structure between the b_{1i} and b_{2i} parameters. At the disk level, we assume b_{1ij} is independent of b_{0ij} and

Table 2. Informative statistical criterion for development of an appropriate height structure by allowing the base parameters to be linear (L) or quadratic (Q) functions of height.

Model	No. of parameters*	Parameter			AIC	BIC	Log-likelihood [†]	LRT [‡]	P-value
		β_0	β_1	β_2					
1	16	Q	Q	Q	8540	8628	-4254.3		
2	15	Q	Q	L	8536	8618	-4253.0	2.6	0.1059
3	14	L	Q	L	8536	8613	-4253.9	1.8	0.1746
4	13	L	L	L	8544	8615	-4259.2	10.4	0.0012
5	13	L	Q		8550	8621	-4262.0		

* The number of parameters includes both the parameters in the mean function (three), variance-covariance parameters (six), a deviance parameter σ , and the appropriate height parameters.

[†] Maximum likelihood method was applied in parameter estimation.

[‡] Likelihood ratio is calculated with respect to the current model and the immediately preceding model.

Table 3. Comparisons of mixed effects model performance with different variance-covariance structures (Diag = Diagonal, Sym = General positive-definite).

Model	No. of parameters	Var-Cov Structure	AIC	BIC	Log-likelihood	LRT*	P-value
3	14	Diag: ψ_1, ψ_2	8536	8613	-4253.9		
4	20	Sym: ψ_1, ψ_2	8526	8636	-4242.9	22.1	0.0012
5	14	Sym: ψ_1	8535	8612	-4327.9	169.9	0.0001

* Likelihood ratio is calculated with respect to the current model and the immediately preceding model

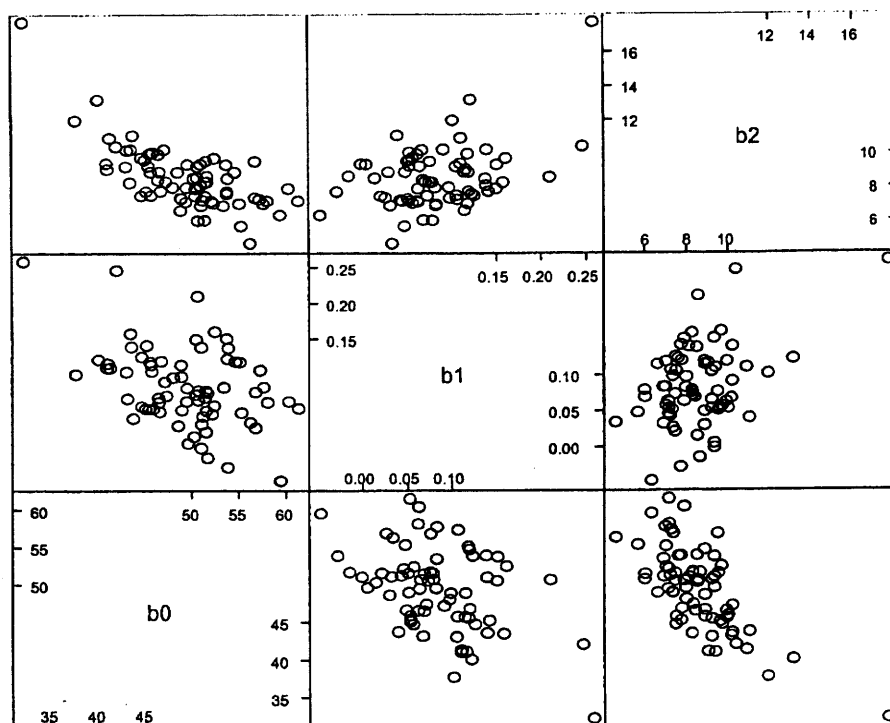


Figure 3. Scatterplot of the estimated random effects from model 4.

b_{2ij} due to low correlation, but allow correlation between b_{0ij} and b_{2ij} .

Determining the Within-Groups Error Structure

The Variance Function

Once the covariates have been determined in the model, we proceed by specifying the variance-covariance structure of the within-group errors to account for heteroskedasticity and autocorrelation. We use a conditional error variance (Davidian and Giltinan 1995, Pinheiro and Bates 2000), where we assume

$$\text{Var}(\epsilon_{ijk}|b_{i,j}, b_{ij}) = \sigma^2 g^2(\mu_{ijk}, v_{ijk}, \delta), \quad (5)$$

where $\mu_{ijk} = E[y_{ijk}|b_{i,j}, b_{ij}]$, v_{ijk} is a vector of variance covariates, δ is a vector of variance parameters, and $g(\cdot)$ is the variance function. The NLME library in S-Plus allows for a wide variety of variance functions (Pinheiro and Bates 2000). Some of the variance structures used include the varIdent, varPower, and varComb functions. The varIdent

class represents a variance model with different variances for each level of stratification, s , that can be represented as

$$\text{Var}(\epsilon_{ijk}) = \sigma^2 \delta_s^2, \quad g(s, \delta) = \delta_s. \quad (6)$$

The varPower structure is given as

$$\text{Var}(\epsilon_{ijk}) = \sigma^2 |v_{ijk}|^{2\delta}, \quad g(v_{ijk}, \delta) = |v_{ijk}|^\delta, \quad (7)$$

which, expanded to account for the levels of early- and latewood stratification, s , becomes

$$\text{Var}(\epsilon_{ijk}) = \sigma^2 |v_{ijk}|^{2\delta_{ijk}}, \quad g(v_{ijk}, s, \delta) = |v_{ijk}|^{\delta_{ijk}}, \quad (8)$$

where δ_{ijk} are the variance parameters for each stratum, s . Finally, the varComb operator allows for combining two or more variance functions. Using these variance structures, we found a varComb variance model corresponding to a variance covariate given by the fitted values by s , but in which the proportionality constant differs according to the level of s , as a product of the varPower and varIdent functions best described these data. The final form of this

Table 4. Comparisons of mixed effects model performance with the addition of covariates (Model 4.1), reduced variance-covariance structure (Model 4.2) and within-groups error structure (Model 4.3).

Model	No. of parameters	AIC	BIC	Log-likelihood	LRT*	P-value
4	20	8526	8636	-4242.9		
4.1	27	7477	7626	-3711.5	1062.7	0.0001
4.2	22	7472	7593	-3714.1	5.2	0.3923
4.3	25	7288	7425	-3619.1	190.0	0.0001

* Likelihood ratio is calculated with respect to the current model and the immediately preceding model.

model's (model 4.2) variance structure is given as

$$\text{Var}(\epsilon_{ijk}) = \sigma^2 |v_{ijk}|^{2\delta_{1s}} \delta_{2s}^2 = \sigma^2 g_1^2(v_{ijk}, s, \delta_1) g_2^2(s, \delta_2). \quad (9)$$

From Table 4, we can see that the addition of the earlywood and latewood covariates (model 4.1) significantly improve on model 4. The LRT statistic comparing the full variance-covariance structure (model 4.1) to the reduced block diagonal structure (model 4.2) was found to be 5.2, with a P-value of 0.39. Comparing models with nested random effects structures via LRTs seems reasonable. However, the usual χ^2 reference distribution is no longer appropriate, falling under the general theory of Wilks' theorem, and results in an overestimated P-value (Pinheiro and Bates 2000). The P-value from this comparison is relatively high, and the log-likelihood values are very similar, indicating that the reduced variance-covariance structure is preferred. The inclusion of an appropriate within-groups error structure (model 4.3) was found to significantly increase the log-likelihood value, and decrease the AIC and BIC values. The LRT value of the proposed error structure with that of the spherical error structure (model 4.2) was found to be 190, with a P-value of 0.0001, indicating a better fit.

Serial Correlation Structure

Correlation structures are used for modeling dependence among observations. In the context of mixed effects models, they are used to model the correlation among the within-subject errors. Correlation structures can be categorized as time series or spatial correlation structures, and the latter can be considered a generalization of the former. The time series correlation structure is most suitable for equally spaced time series data or equally spaced distance data. If we use vector p_{ijk} to denote the position vector of within-subject error ϵ_{ijk} and model the within-subject correlation of ϵ_{ijk} and ϵ'_{ijk} as a function of relative distance between p_{ijk} and $p\epsilon'_{ijk}$, then the correlation of the errors can be defined as $\text{corr}(\epsilon_{ijk}, \epsilon'_{ijk}) = h[d(p_{ijk}, p_{ijk}'), \rho]$, where ρ are correlation parameters and $h(\cdot)$ is a specified correlation function. Times series correlation structures may only work if the p_{ijk} are integer scalars, but a spatial correlation structure has no such restrictions. For our data, we have approximately equally spaced MFA measurements taken at 3-meter intervals along the tree stem, so a time series correlation structure may be used to approximate MFA autocorrelation within a tree.

For sample data, we can use an empirical autocorrelation function (Box et al. 1994) to estimate the serial correlation, and gain insight into choosing an appropriate correlation

structure. The empirical autocorrelation at lag l as defined by Pinheiro and Bates (2000) is

$$\hat{\rho} = \frac{\sum_{i=1}^M \sum_{j=1}^{M_i} \sum_{k=1}^{n_{ij}-1} r_{ijk} r_{ij(k+l)} / N(l)}{\sum_{i=1}^M \sum_{j=1}^{M_i} \sum_{k=1}^{n_{ij}} r_{ijk}^2 / N(0)}, \quad (10)$$

where $N(l)$ is the number of residual pairs used in the summation defining the numerator of $\hat{\rho}(l)$, and r_{ijk} is the standardized residuals in the mixed-effects model. An approximated two-sided critical value for the empirical autocorrelation $\hat{\rho}(l)$ at significance level α can be calculated as $Z_{(1-\alpha/2)} \sqrt{N(l)}$, where $Z_{(1-\alpha/2)}$ is the standard normal quantile at $1 - \alpha/2$. A plot of the estimated autocorrelation coefficients against lags with critical value boundary lines at the 0.05 level for model 4.3 is given in Figure 4. At lag 1, the empirical correlation coefficient is positive, indicating that two adjacent MFA disk measurements are similar to a certain extent. The empirical correlation coefficients at all other lags are negative, which is against intuition. This counterintuitive autocorrelation is not uncommon and is symptomatic of the complexity of within-errors autocorrelation (Davidian and Giltinan 1995, Fang and Bailey 2001).

A host of correlation structures are available to account for the within-tree autocorrelation. The simplest is a compound symmetry model, which assumes equal correlation among all measurements within the same tree. However, a compound symmetric structure may be too simplistic,

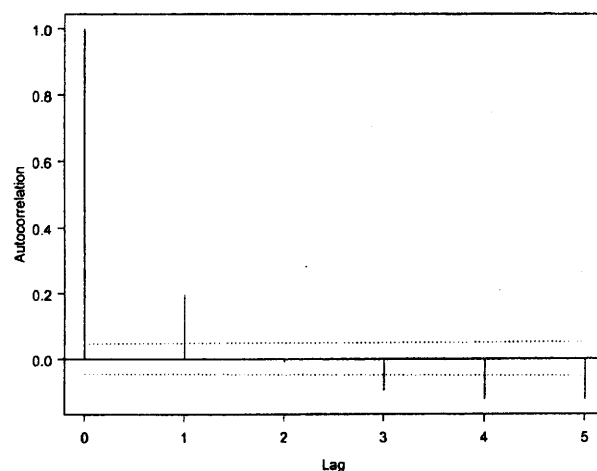


Figure 4. Scatterplot of empirical autocorrelation versus lag from model 4.3.

because we expect that correlation decreases with an increase of absolute disk distance. Another general class of correlation structures is the autoregressive-moving average model, also known as ARMA models (Box et al. 1994). This family of correlation structures is a mixture of an autoregressive model and a moving average model.

An autoregressive model, AR(\cdot), defines the current within-subject error as a linear function of the previous within-subject errors plus a homoskedastic noise term with expected value 0. This can be written as

$$\varepsilon_t = \phi_1 \varepsilon_{t-1} + \dots + \phi_p \varepsilon_{t-p} + a_t \quad (11)$$

The number of past residual errors in the model, p , is called the order of the autoregressive model. When p equals 1, Equation 11 reduces to an AR(1) correlation structure.

The moving average correlation model, MA(\cdot), assumes the current within-subject error is a linear function of the last several independent and identical distributed within-subject errors plus a noise term, and is defined as

$$\varepsilon_t = \theta_1 a_{t-1} + \dots + \theta_q a_{t-q} + a_t \quad (12)$$

As in the autoregressive model, q in Equation 12 is called the order of the moving average model.

The ARMA(p, q) model is a mixture of a p -order autoregressive and q -order moving average models, with $p + q$ parameters, and is given as

$$\varepsilon_t = \sum_{i=1}^p \phi_i \varepsilon_{t-i} + \sum_{j=1}^q \theta_j a_{t-j} + a_t \quad (13)$$

Differing correlation structures were fit to model 4.3 (Table 5), and we used LRTs, AIC, and BIC criteria for determining the best correlation structure for the within-subject errors. It can be seen that the added correlation structures greatly improve on model 4.3. AIC, BIC, and log-likelihood values all confirm that an AR(1) model (model 4.3.1) is the best correlation structure. Model 4.3.1 has the lowest AIC and BIC values and the fewest parameters. Further analysis utilizing LRTs comparing model 4.3.1 versus the other correlation structures indicated no significant difference in the models, reassuring that the parsimonious AR(1) model should be selected. The estimated empirical correlation coefficients for Model 4.3.1 were found to be

$$\hat{\rho} = [\hat{\rho}(1), \hat{\rho}(2), \hat{\rho}(3), \hat{\rho}(4), \hat{\rho}(5)]^T \\ = [-0.0482, -0.0054, -0.0394, -0.05911, -0.6956]^T.$$

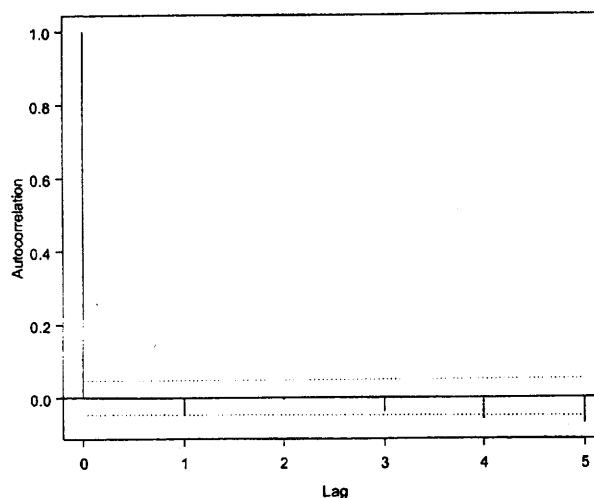


Figure 5. Scatterplot of empirical autocorrelation versus lag from model 4.3.1 with an AR(1) correlation structure.

Figure 5 is a graph of the empirical autocorrelation coefficients versus lags for the transformed within-subject errors. The transformed within-subject errors appear to be uncorrelated noise with negligible empirical autocorrelation coefficient, except at lags 4 and 5, at which the estimated autocorrelation coefficients are greater than their critical values. This may be due to a small sample size or unreliability of empirical autocorrelation calculation at high lags. The AR(1) correlation structure sufficiently accounts for dependency among repeated MFA measurements from the same tree. The coefficient of the AR(1) correlation structure from model 4.3.1 was found to be 0.3373, and the autocorrelation function is

$$h(k, \phi) = \phi^k, \quad k = 0, 1, \dots \quad (14)$$

Accounting for the correlation of the within-groups errors may also change the variance-covariance correlation of the estimated random effects. On closer inspection of model 4.3.1, it was decided that the variance-covariance structure of Ψ_1 could be simplified by assuming an independent block diagonal matrix due to the low correlation between the b_{1i} and b_{2i} parameters. Attempts were also made to simplify the variance-covariance matrices of both Ψ_1 and Ψ_2 by dropping the least-significant random effects parameters. However, doing this resulted in a significant reduction in log-likelihood and an increase in AIC and BIC values.

Table 5. Comparisons of mixed effects model performance with different within-groups correlation structures.

Model	Correlation structure	No. of parameters	AIC	BIC	Log-likelihood	LRT*	P-value
4.3	Independent	25	7288	7425	-3619.1		
4.30.1	AR(1)	26	7149	7292	-3548.6	140.9	0.0001
4.30.2	MA(1)	26	7169	7312	-3558.5	121.1	0.0001
4.30.5	MA(2)	27	7152	7300	-3549.1	140.1	0.0001
4.30.6	AR(2)	27	7151	7299	-3548.5	141.1	0.0001
4.30.3	ARMA(1,1)	27	7151	7299	-3548.6	140.9	0.0001
4.30.4	ARMA(1,2)	28	7151	7305	-3547.8	142.5	0.0001

* Likelihood ratio is calculated with respect to Model 4.3.

LRT values indicated that the only appropriate simplification was by specifying the block diagonal structure in Ψ_1 , which can be specified as

$$\text{Var}(b_i) = \text{Var} \begin{pmatrix} b_{0i} \\ b_{1i} \\ b_{2i} \end{pmatrix} = \Psi_1 = \begin{pmatrix} 0 & 0 & 0 \\ 0 & \psi_{11} & 0 \\ 0 & 0 & \psi_{22} \end{pmatrix}.$$

An LRT indicated that the reparameterization of Ψ_1 from model 4.3.1 was justified. The P -value of the LRT was found to be 0.4767, and the new model has parameters, AIC, BIC, and log-likelihood values of 25, 7,147, 7,285, and $-3,548.8$, respectively.

Interpretation of Model Parameters

With the variance-covariance matrices, within-group errors, and autocorrelation functions specified, it is now possible to reduce the full model in Equation 4 by removing insignificant fixed-effects parameters. The β_{21} parameter was found to be the only highly insignificant fixed-effects parameter in the model, and was subsequently dropped and the model refitted. Fit index values for the model were found to be 0.81, 0.86, and 0.92 at the population, tree, and disk levels, respectively. Diagnosis of the final model can also be accomplished by inspection of a plot of the residuals versus fitted values (Figure 6). Smoothing techniques are useful to evaluate the possible bias across fitted values. The kernel smoother used is

$$\hat{y}_i = \sum_{j=1}^n y_j K \left(\frac{x_i - x_j}{b} \right) / \sum_{j=1}^n \left(\frac{x_i - x_j}{b} \right), \quad (15)$$

where b is the bandwidth parameter and K is a kernel function. The critical parameter is the bandwidth parameter b , which determines computing time and the degree of detail derived from the smoothing application. A bandwidth of 1 was chosen, and the kernel function is a standard normal distribution. Figure 6 does not indicate any general trends or patterns, and overall the standardized residuals are small, suggesting that the final model was successful in explaining the variation of MFA.

It is possible to obtain population or "typical" prediction values of earlywood and latewood MFA by setting the random effects estimates to 0, and substituting corresponding fixed-effects values into Equation 4. Parameter estimates and corresponding standard errors and P -values for the fixed effects of the reduced model are given in Table 6. We constructed a plot of the population, or "typical" MFA for earlywood and latewood at heights of 1.4, 4.6, 7.6, 10.7, and 13.7 meters (Figure 7). Initial values at all heights were found to be greater for earlywood than latewood. Similarly, the lower asymptotic bounds reached at each height level were found to be greater in earlywood than latewood.

From Table 6, one can evaluate the fixed-effects model parameters at differing height values. At a height of 1 meter, which sets the value of height in the model to 0, the initial value, rate, and lower asymptote parameters for earlywood and latewood, respectively, were found to be 49.9114 and 46.4387, 0.0649 and 0.0357, and 9.1290. The initial values of earlywood will always be larger at any height than those of latewood. The initial rate of change of MFA was found to be higher in earlywood. However, because the rate parameter changes with disk height, it was found that, at a

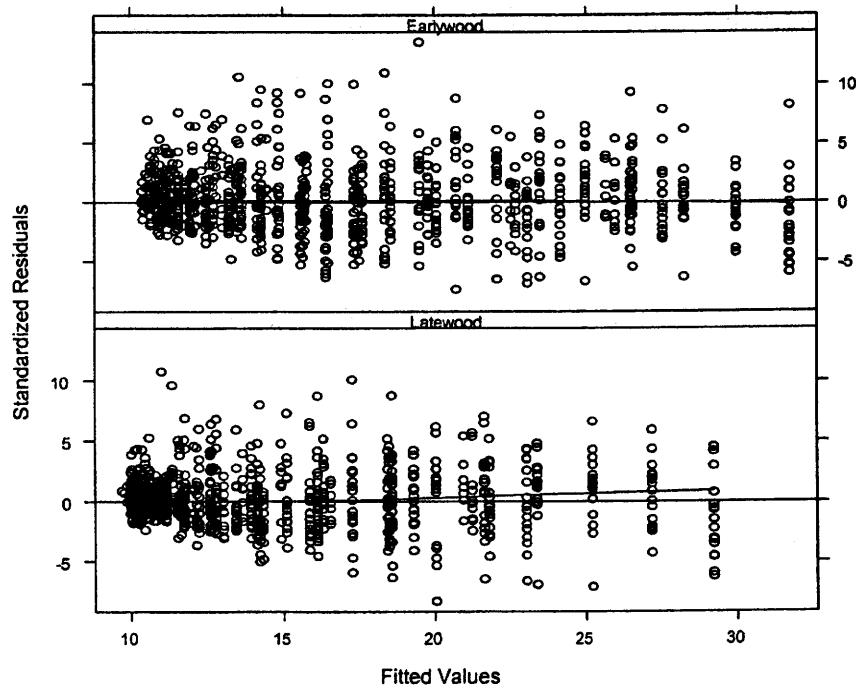


Figure 6. Plot of standardized residuals versus fitted values with a loess smoother for the reduced modified logistic microfibril angle model with random effects and AR(1) within-groups autocorrelation and power variance function proportional to stratification.

Table 6. The estimated parameters for population prediction of earlywood and latewood microfibril angle (random effects input as 0) with the modified Logistic function.

Parameter	Estimate	Std. Error	P-value
β_{00}	49.9114	1.9732	0.0001
β_{01}	-3.4736	1.8310	0.0580
β_{02}	-5.4636	1.1533	0.0001
β_{03}	-2.4039	1.1223	0.0323
β_{10}	0.0649	0.0269	0.0159
β_{11}	-0.0291	0.0136	0.0330
β_{12}	0.2794	0.0495	0.0001
β_{13}	0.2504	0.0431	0.0001
β_{14}	-0.0598	0.0186	0.0014
β_{15}	-0.0892	0.0169	0.0001
β_{20}	9.1290	0.4629	0.0001
β_{22}	0.8207	0.2527	0.0012
β_{23}	-0.2614	0.1129	0.0207

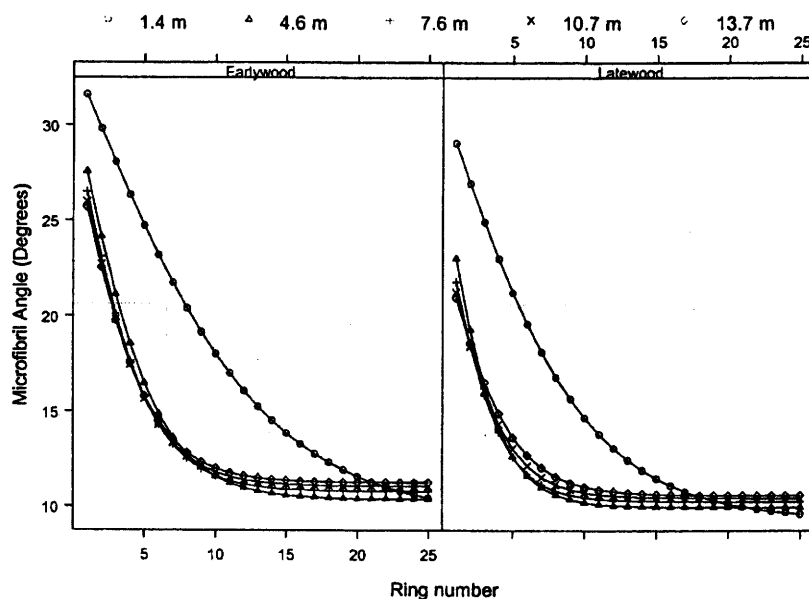


Figure 7. A comparison of the mean responses (typical responses) of microfibril angle by wood type and height level (m).

height of ~1.13 meters, the rate of change of earlywood and latewood MFA is roughly equivalent. Above 1.13 meters, latewood MFA decreases faster than earlywood until a height of ~14.66 meters, where the rate of change of earlywood and latewood are roughly equivalent. Above 14.66 meters, earlywood MFA decreases at a faster rate than latewood MFA. It should be noted that 14.66 meters is well outside the natural range of the data, and caution should be used in interpretation. The asymptotic bounds for earlywood and latewood are the same at a height of 1 meter, however the bounds become larger with increasing disk height, and earlywood MFA will always have a larger asymptotic bound than latewood. Even though it has been shown that population predictions from the final model accurately describe the trends of earlywood and latewood MFA, inclusion of the random effects estimates will allow for more precise prediction. As a comparison, we graphed the predictive curves with and without random effects for a single tree in the original data set. From this, it can be seen

that more precise predictions are obtained with the inclusion of the estimated random effects in the model (Figure 8).

Cross-Validation and Model Diagnosis

The model diagnosis techniques described above rely strictly on residual values from the fitted data. This approach has an inherent limitation, given that the same data were used both for fitting and model diagnosis. The main application of our model is earlywood and latewood MFA prediction for trees not in our fitting data set. The use of data-splitting or cross-validation has been shown not to provide any additional model information compared to the statistics obtained from models fit to the entire data set (Kozak and Kozak 2003). Models validated with an independent data set prove that either the data are from the same population and will perform as per se validation using data-splitting or the data are from a different population entirely, in which case the models should be refit to obtain more appropriate parameter estimates. However, cross-

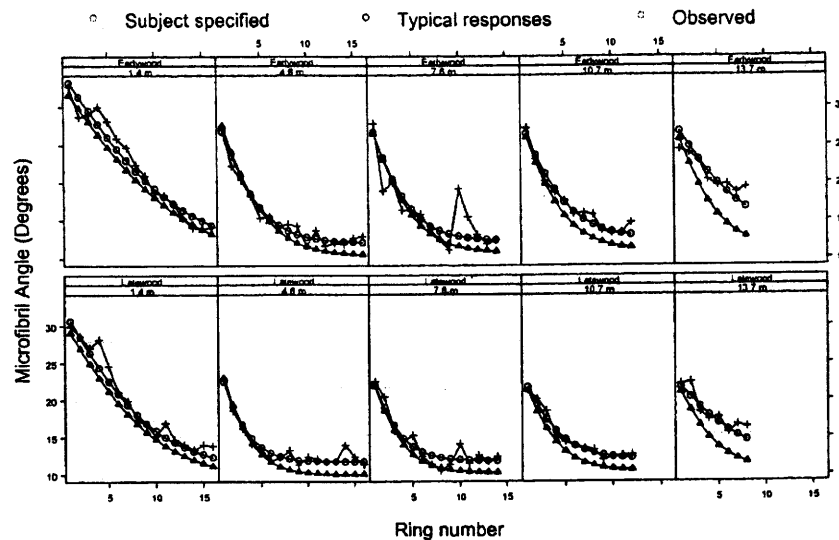


Figure 8. A comparison of individual microfibril angle predictions by typical response and subject-specified response with the final reduced nonlinear mixed-effects microfibril angle model.

validation is a useful tool for evaluating the stability and functional form of the models presented above and will be used here to verify the intrinsic flexibility of the models. Because of the independence between the fitting data and the validation data sets, the degree of accuracy of MFA predictions from the validation data set to the true observed values is a good indication of model performance. To preserve the original hierarchical data structure, the fitting data set was constructed by first randomly selecting 14 of the 18 sampled trees along with their corresponding variables of interest, leaving 4 trees to be used for model validation.

Cross-validation model diagnosis can be used to assess overall model bias, bias at different heights, bias at different ring numbers from the pith, and the overall variation of the residuals. Residuals are calculated as the differences between the observed and predicted MFA values. Fit statistics from the validation data set are presented in Table 7. Fit index values at the population level were found to be 0.81 across earlywood and latewood, 0.78 for earlywood, and 0.81 for latewood, respectively. The mean residual values at all levels were found to be positive, indicating that the model is underestimating MFA. Figure 9 validates that the model is yielding relatively accurate ring MFA prediction, and overall prediction is unbiased because the mean bias is small. The majority of the standardized residuals versus fitted values are centered on zero, with no obvious patterns.

Table 7. Fit statistics from cross-validation including fit index (FI), mean residual (MRS), absolute mean residual (AMRS), and root mean square error of prediction (RMSEP) at the population level across strata (Early/Late) and by strata (Earlywood, Latewood).

Fit Statistic	Level		
	Early/Late	Earlywood	Latewood
FI	0.81	0.78	0.81
MRS	0.25	0.14	0.37
AMRS	1.98	2.17	1.79
RMSEP	2.49	2.74	2.23

Graphical analysis and smoothing techniques were conducted to evaluate model bias at differing ring numbers and heights. The scatterplot of residuals versus ring number will reveal possible bias at different ring numbers. In the same vein, the scatterplot of residuals versus relative height can be used to assess bias in the longitudinal direction. Scatterplots of the residuals versus ring number and the natural log of disk height with their corresponding smoothing lines are found in Figures 10 and 11. The points are almost symmetric around zero on the scatterplot of residuals versus ring number, and its smoothing line almost overlaps the x axis. However, there does appear to be a mild quadratic trend. Thus, the model is overall unbiased across ring number. In the plot of residuals versus the natural log of disk height, there appears to be extreme bias at larger disk heights, indicating that the model is underestimating the true MFA.

Prediction for New Observations

MFA prediction is a major application of this model. Accurate MFA predictions can improve wood quality prediction and utilization. The nonlinear mixed effects model allows for the prediction of MFA from trees that may or may not have prior measured observations.

Case 1: Prediction Is Required for a New Tree with No Prior Observations

If no prior information is available for an individual tree, it is impossible to determine the random effects for the tree. The only choice is to use the random effects expected values, which are zero by definition. The model simply reduces to the population level model and we can predict MFA at the k th ring from pith at the j th height level as

$$\widehat{\text{MFA}}_{jk} = \frac{\hat{\beta}_{0jk}}{1 + e^{\hat{\beta}_{1jk}}} + \hat{\beta}_{2jk}$$

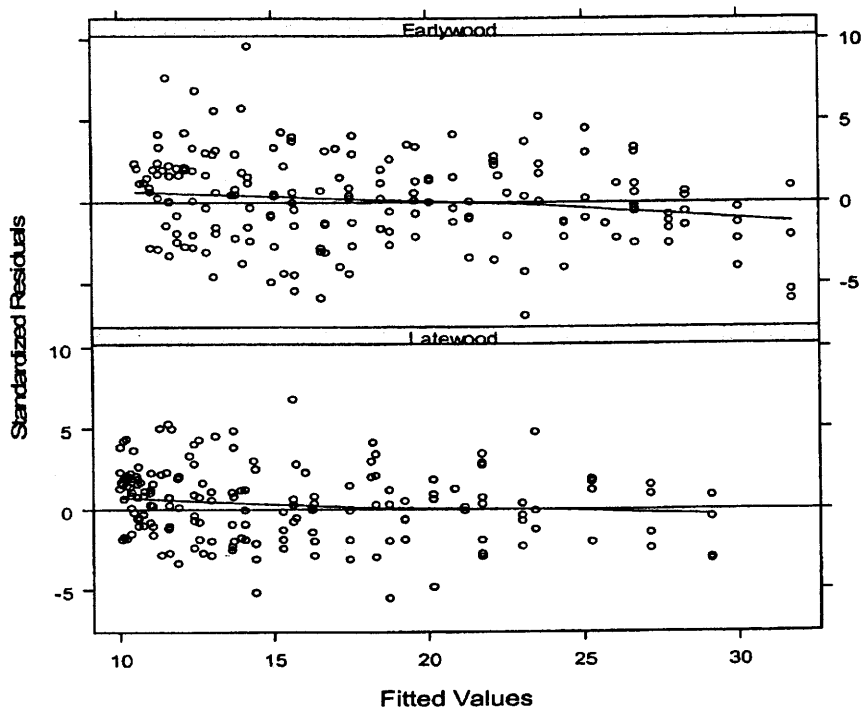


Figure 9. Plot of standardized residual versus fitted values with a loess smoother for cross-validation of the reduced modified logistic microfibril angle model with random effects and AR(1) within-groups autocorrelation and power variance function proportional to stratification.

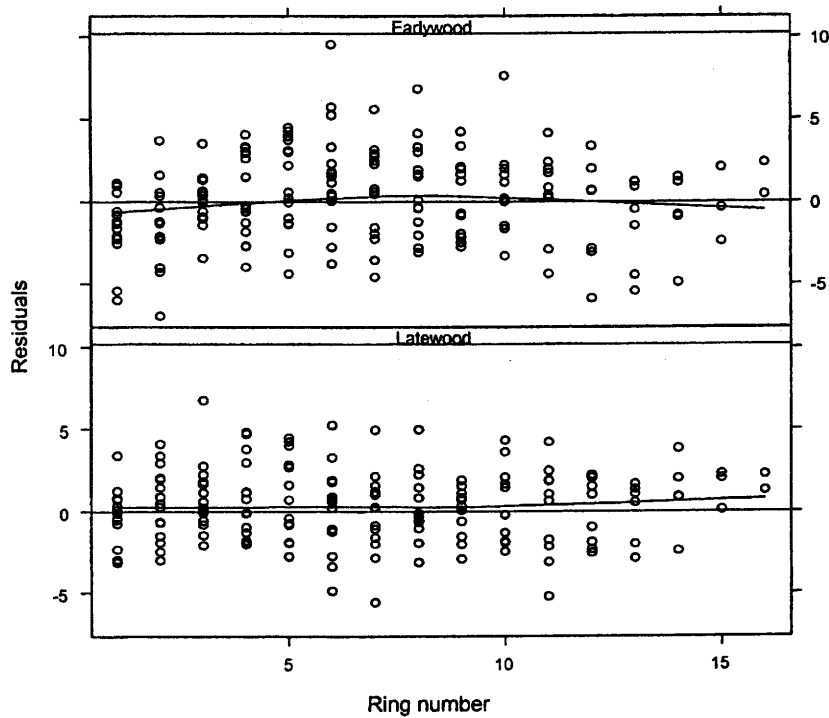


Figure 10. Plot of residuals versus ring number with a loess smoother for cross-validation of the reduced modified logistic microfibril angle model with random effects and AR(1) within-groups autocorrelation and power variance function proportional to stratification.

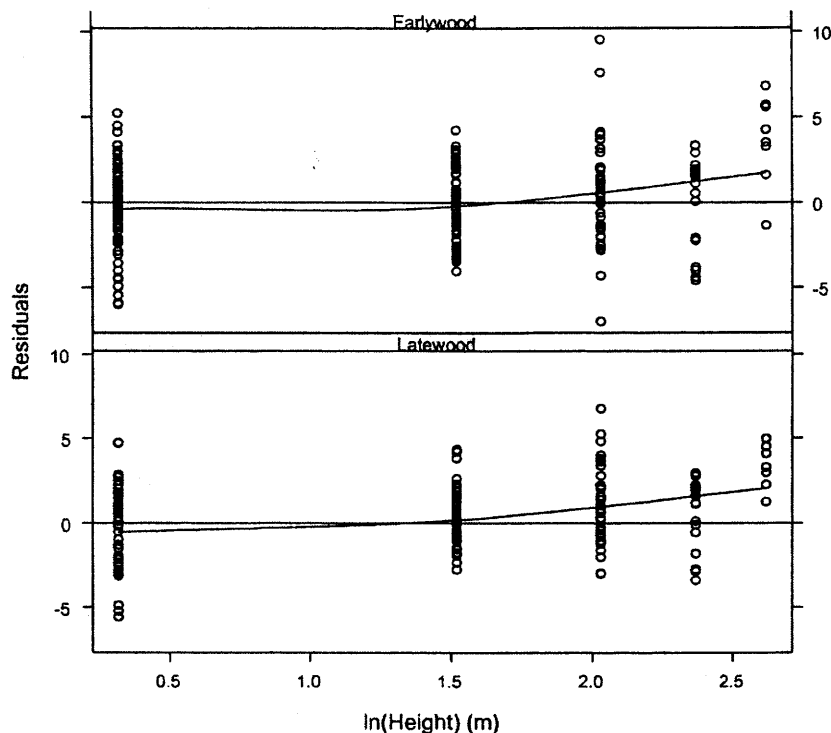


Figure 11. Plot of residuals versus the natural log of disk height with a loess smoother for cross-validation of the reduced modified logistic microfibril angle model with random effects and AR(1) within-groups autocorrelation and power variance function proportional to stratification.

where

$$\hat{\beta}_{jk} = (\hat{\beta}_{0jk} \hat{\beta}_{1jk} \hat{\beta}_{2jk})^T = A_{jk}\beta^T,$$

β^T

$$= (\hat{\beta}_{00} \hat{\beta}_{01} \hat{\beta}_{02} \hat{\beta}_{03} \hat{\beta}_{10} \hat{\beta}_{11} \hat{\beta}_{12} \hat{\beta}_{13} \hat{\beta}_{14} \hat{\beta}_{15} \hat{\beta}_{20} \hat{\beta}_{22} \hat{\beta}_{23})^T,$$

$$A_{jk} = \begin{pmatrix} 1 & I_x & \ln(ht_{jk}) & \ln(ht_{jk})I_x & 0 & 0 & 0 \\ 0 & 0 & 0 & 0 & 1 & I_x & \ln(ht_{jk}) \\ 0 & 0 & 0 & 0 & 0 & 0 & 0 \end{pmatrix},$$

$$\begin{pmatrix} 0 & 0 & 0 & 0 & 0 & 0 & 0 \\ \ln(ht_{jk})I_x & \ln\{(ht_{jk})\}^2 & \ln\{(ht_{jk})\}^2 I_x & 0 & 0 & 0 & 0 \\ 0 & 0 & 0 & 1 & \ln(ht_{jk}) & \ln(ht_{jk})I_x \end{pmatrix},$$

$$B_1 = \begin{pmatrix} 0 & 0 & 0 \\ 0 & 1 & 0 \\ 0 & 0 & 1 \end{pmatrix}, \quad B_2 = \begin{pmatrix} 1 & 0 & 0 \\ 0 & 1 & 0 \\ 0 & 0 & 1 \end{pmatrix}.$$

Taking the first-order expansion of MFA at $\beta = \hat{\beta}$, we can obtain the prediction variance,

$$\text{var}(\text{MFA}_{jk} - \widehat{\text{MFA}}_{jk})$$

$$= F_{jk}^T(\hat{\beta}_{jk})(A_{jk}\hat{\Omega}A_{jk}^T + B_1\hat{\Psi}_1B_1^T + B_2\hat{\Psi}_2B_2^T) \cdot F_{bjk}(\hat{\beta}_{jk}) + \hat{\sigma}^2\hat{R}_{jk}, \quad (16)$$

where Ψ_1 is a 3×3 covariance matrix for the tree level random effects, Ψ_2 is a 3×3 covariance matrix for the disk level random effects, \hat{R}_{jk} is scalar for the variance of the

error term, and $\hat{\Omega}$ is a 13×13 covariance matrix of the estimated parameter vector β ,

$$F_{jk}^T(\hat{\beta}_{jk}) = \left. \frac{\partial f(\text{Ring}_{jk}, \beta_{jk})}{\partial \beta_{jk}} \right|_{\beta_{jk} = \hat{\beta}_{jk}}.$$

With the above formulas, one can estimate ring MFA, the prediction variance, and corresponding confidence intervals. An approximate $100(1 - \alpha)$ confidence interval for this prediction is given as

$$\text{MFA}_{jk} \pm t(n - p - q + 1, 1 - \alpha/2) \sqrt{\text{var}(\text{MFA}_{jk})},$$

where n is the total number of observations, p is the total number of fixed effects parameters, and q is the number of the j th level random effects. As an example, consider estimating earlywood MFA at ring number 3 from pith at a height of 1.37 meters aboveground. The predicted value is 28.24 with variance of 15.70 and corresponding confidence intervals of [20.47, 36.01] at the $\alpha = 0.05$ level.

Case 2: Prediction for a New Tree with Incremental Core Measurements

Oftentimes, accurate MFA estimates are required not for a single tree, but for a plot, stand, or plantation. In this case, the population level prediction may be inadequate. One alternative is to draw several incremental cores at various

heights from a sample of trees and determine the ring-by-ring earlywood and latewood MFA of the incremental cores. These ring values can then be used to obtain an estimate of the tree random effects, which can then be averaged to estimate the mean random effects response in the stand, potentially improving prediction.

Suppose j incremental cores are selected from i trees in a plantation for earlywood and latewood MFA analysis. The number of rings of the j th incremental core from the i th tree is M_i . Let y_{ijk} equal the response at the measurement of the k th ring from pith on the j th increment core of the i th tree. This can be expressed as

$$y_{ijk} = f(\beta_{ijk}, v_{ijk}), \varepsilon_{ijk}, \quad (18)$$

where $i = 1, \dots, M, j = 1, \dots, M_i, k = 1, \dots, n_{ij}$. Population level MFA predictions are given as

$$\text{MFA}_{ijk} = \frac{\hat{\beta}_{0ijk}}{1 + e^{\hat{\beta}_{1ijk}}} + \hat{\beta}_{2ijk},$$

with $\hat{\beta}_{0ijk}$, $\hat{\beta}_{1ijk}$, and $\hat{\beta}_{2ijk}$ defined similarly to case 1 MFA prediction.

We can estimate the random effects of tree i as

$$\hat{b}_i = (\hat{b}_{1i}, \hat{b}_{2i})^T = D_{i,1} Z_{i,1}^T \sum_i^{-1} (y_i - \hat{y}_i), \quad (19)$$

where y_{ijk} is the response vector of the i th tree and \hat{y}_i is the corresponding population level prediction,

$$\begin{aligned} \hat{\Sigma}_i &= (Z_{i,1,1} \hat{\Psi}_1 Z_{i,1,1}^T + Z_{i,1,2} \hat{\Psi}_2 Z_{i,1,2}^T + \hat{R}_{i1}) \\ &\oplus (Z_{i,2,1} \hat{\Psi}_1 Z_{i,2,1}^T + Z_{i,2,2} \hat{\Psi}_2 Z_{i,2,2}^T + \hat{R}_{i2}) \oplus \dots \\ &\oplus (Z_{i,M_i,1} \hat{\Psi}_1 Z_{i,M_i,1}^T + Z_{i,M_i,2} \hat{\Psi}_2 Z_{i,M_i,2}^T + \hat{R}_{iM_i}), \end{aligned}$$

$$Z_{ijk,1} = \frac{\partial f(\text{ring}_{ijk}, \ln(Ht_{ijk}), \beta_{ij})}{\partial \beta_{ij}} B_1,$$

$$Z_{ijk,2} = \frac{\partial f(\text{ring}_{ijk}, \ln(Ht_{ijk}), \beta_{ij})}{\partial \beta_{ij}} B_2,$$

\hat{R}_{ij} is an $n_{ij} \times n_{ij}$ within-disk variance-covariance matrix of the j th disk from the i th tree, and all other variables previously defined.

The value of MFA of tree i , at height j , and ring k , is given as

$$\begin{aligned} Z_{ij,1} &= (Z_{ij,1,1}, Z_{ij,2,1}, \dots, Z_{ij,n_{ij},1})^T, \\ Z_{ij,2} &= (Z_{ij,1,2}, Z_{ij,2,2}, \dots, Z_{ij,n_{ij},2})^T, \end{aligned} \quad (20)$$

Variance for prediction at the k th ring on the j th increment core of the i th tree is

$$\text{MFA}_{ijk} = \frac{\hat{\beta}_{0ij}}{1 + \exp(\hat{\beta}_{1ij} + \hat{b}_{1i})} + \hat{\beta}_{2ij} + \hat{\beta}_{2i}, \quad (21)$$

where,

$$\begin{aligned} \text{var}(y_{ijk} - \hat{y}_{ijk}) &= F_{ijk}^T(\hat{\beta}_{ij}) \hat{\Omega}(\hat{\beta}_{ijk}) F_{ijk}(\hat{\beta}_{jk}) \\ &+ \hat{Z}_{ijk,2}^T \hat{\Psi}_2 \hat{Z}_{ijk,2} + \hat{Z}_{ijk,1}^T \hat{\Psi}_1 \hat{Z}_{ijk,1} \\ &+ \hat{F}_{ijk}^T(\hat{\beta}_{ijk}) \hat{C}_i \hat{Z}_{ijk,1} \\ &+ \hat{Z}_{ijk,1}^T \hat{C}_i^T \hat{F}_{ijk}(\hat{\beta}_{ijk}) + \hat{R}_{ijk}, \end{aligned} \quad (22)$$

where,

$$\begin{aligned} \hat{\Omega}(\hat{\beta}_{ijk}) &= A_{ijk} \hat{\Omega} A_{ijk}^T, \\ \hat{V}_i &= \hat{\Psi}_1 - \hat{\Psi}_1 \hat{Z}_{i,1}^T \hat{\Sigma}_i^{-1} Z_{i,1} \hat{\Psi}_1 + \hat{\Psi}_1 Z_{i,1}^T \hat{\Sigma}_i^{-1} \\ &\cdot F(\hat{\beta}) \Omega(\hat{\beta}_{ijk}) F^T(\hat{\beta}) \hat{\Sigma}_i^{-1} Z_{i,1} \hat{\Psi}_1, \\ \hat{C} &= \text{Cov}[(\hat{\beta}_{ij} - \beta_{ij}), (\hat{b}_{i,1} - b_{i,1})] \\ &= -\Psi(\hat{\beta}_{ijk}) \hat{F}^T(\hat{\beta}) \hat{\Sigma}_i^{-1} Z_{i,1} \hat{\Psi}_1, \\ Z_{i,1} &= (Z_{i,1,1}, Z_{i,2,1}, \dots, Z_{i,M_i,1})^T, \end{aligned}$$

and all other variables previously defined.

As an example, if one were to take an incremental core at 1.37 meters aboveground that has 16 rings, with corresponding earlywood MFA measurements of $y = (32.71, 28.70, \dots, 14.13)^T$. From Equations 19, the tree level random effects estimators are $\hat{b}_i = (0, -0.0032, -0.0655)^T$. Applying Equations 21 and 22 yields an earlywood MFA prediction of 27.70, variance of 11.69, and confidence intervals of [20.99, 34.40] at the $\alpha = 0.05$ level. We can see that the case 2 prediction has a smaller variance, thus higher precision.

Discussion and Conclusions

Mixed effects models are useful tools for analyzing repeated measures data. Their inherent flexibility allows for development of a unique variance-covariance structure, which is limiting in traditional nonlinear regression. A variant of the logistic function is used to characterize these patterns. Ring number from pith and the natural logarithm of disk height were found to be good predictor variables and were incorporated into the model. The incorporation of the disk height predictor variables into the model was accomplished by making the parameters of the logistic function linear functions of height. The analysis results show that a mixed-effects model provides more accurate predictions and an overall better fit.

A random-effects model may alleviate the problems of nonconstant variance and autocorrelation among the repeated measurements. The final model has two levels of mixed effects with random effects at the tree and disk levels. Autocorrelation was accounted for in this model by assuming that the disk error term was from an AR(1) process. Heteroskedasticity was accounted for with a variance model corresponding to a variance covariate given by the fitted values for each wood type, but in which the proportionality

constant differs according to the level of wood type, was identified as the within-group variance structure.

The mixed-effects model was found to be underestimating the true value of MFA at the population level, and by wood type. Overall, the model was found to be unbiased across ring number, with a mild quadratic trend observed in the plot of residuals versus the natural logarithm of disk height. It should be noted that, of the 18 trees used in this analysis, only 7 trees were tall enough to have disks removed at 13.7 meters. From these 7 trees there were a total of 118 ring observations, for an average number of 8.4 earlywood and latewood rings per tree. The bias of the model at upper heights may possibly be overcome by fitting to a more complete data set, properly calibrating the model.

The population level MFA model is suitable for prediction of earlywood and latewood MFA for a population of trees. One way to attain better MFA predictions is to estimate random effects by determining ring-by-ring MFA values from incremental cores taken from several sample trees. These estimated random effects will allow better prediction precision. This approach can be useful for predicting MFA values of a unique stand or plantation. Several trees from such a stand can be selected and felled for MFA analysis. Each of these trees will yield unique tree and disk level random effects estimates, and the mean of these random effects can be used to adjust the MFA prediction for that stand or plantation.

The random effects estimates were found to be larger at the second level or disks within a tree level, thus accounting for more variation. This means that the MFA values from tree to tree are relatively consistent, but the disks within a tree exhibit more variation, due to the unique patterns of MFA corresponding to height level. MFA should be more similar in trees sampled from within the same stand. We attempted to incorporate between-tree spatial correlation into these models by adding a stand level effect. However, the addition of this random effect did not significantly improve model performance. This may appear counterintuitive to logic, but it may be the case that environmental impacts have negligible influence on MFA compared to the genetic makeup, size, and position the tree holds within the stand, i.e., dominant, co-dominant, or suppressed.

It should be recognized that the data used in this study were collected from trees in stands with similar site indices, growing conditions, ages, and size characteristics from within a narrow geographic range, severely restricting the use of the model. Thus, caution should be used when extrapolating beyond the natural range of the data on which the model is based. However, the models presented in this article provide prototypes from which data collected in other regions, or for a larger more inclusive data set, could be based.

Literature Cited

- ADDIS, T., A.H. BUCHANAN, AND J.C.F. WALKER. 1995. A comparison of density and stiffness for predicting wood quality. Or density: The lazy man's guide to wood quality. *Journal of the Institute of Wood Science* 13(6):539-543.
- BAILEY, R.L., AND J.L. CLUTTER. 1974. Base-age invariant polymorphic site curves. *For. Sci.* 20:155-159.
- BOX, G.E.P., G.M. JENKINS, AND G.C. REINSEL. 1994. *Time series analysis: Forecasting and control*, 3rd ed., Holden-Day, San Francisco.
- CAVE, I.D., AND J.C. F. WALKER. 1994. Stiffness of wood in fast-grown plantation softwoods: The influence of microfibril angle. *Forest Products Journal* 44(5):43-48 p.
- CLARK, A., B. BORDERS, AND R. DANIELS. 2004. Impact of vegetation control and annual fertilization on properties of loblolly pine wood at age 12. *Fors. Prod. J.* 54(12):90-96 p.
- CLUTTER, J.L. 1961. The development of compatible analytic models for growth and yield of loblolly pine. PhD dissertation, Duke University, Durham, NC.
- DANIELS, R.F., R. HE, A. CLARK III, AND R. SOUTER. 2002. Predicting wood properties of loblolly pine from stump to tip and pith to bark. *In* Proceedings of the fourth workshop. Connection between forest resources and wood quality: Modelling approaches and simulation software, Nepveu, G. (ed.). IUFRO working party S5.01-04. Harrison Hot Springs, B.C. CA. Sept 8-14, 2002. INRA-Centre de Recherches de Nancy, France.
- DAVIDIAN, M., AND D. M. GILTINAN. 1995. *Nonlinear models for repeated measurement data*. Chapman and Hall, London, UK.
- FANG, Z., AND R.L. BAILEY. 2001. Nonlinear mixed effects modeling for slash pine dominant height growth following intensive silvicultural treatments. *For. Sci.* 47(3):287-300.
- GREGOIRE, T.G., O. SCHABENBERGER, AND J.P. BARRETT. 1995. Linear modeling of irregularly spaced, unbalanced, longitudinal data from permanent-plot measurements. *Can. J. For. Res.* 25:137-156.
- HALL, D.B., AND M. CLUTTER. 2004. Multivariate multilevel nonlinear mixed effects models for timber yield predictions. *Biometrics* 60:16-24.
- KELLOGG, R.M., E. THYKESON, AND W.G. WARREN. 1975. The influence of wood and fiber properties on kraft converting-paper quality. *Tappi* 58(12):113-116.
- KOZAK, A., AND R. KOZAK. 2003. Does cross validation provide additional information in evaluation of regression models? *Can. J. For. Res.* 33:976-987.
- LAPPI, J., AND R.L. BAILEY. 1988. A height prediction model with random stand and tree parameters: An alternative to traditional site index methods. *For. Sci.* 38(2):409-429.
- LARSON, P.R., D.E. KRETSCHMANN, E. DAVID, A. CLARK, AND J.G. ISEBRANDS. 2001. Formation and properties of juvenile wood in southern pines: A synopsis. Gen. Tech. Rep. FPL-GTR-129. USDA Forest Service, Forest Products Lab., Madison, WI. 42 p.
- LICHTENEGGER, H., A. REITERER, S.E. STANZL-TSCHEGG, AND P. FRATZL. 1999. Variation of cellulose microfibril angles in softwoods and hardwoods—A possible strategy of mechanical optimization. *J. Struct. Biol.* 128:257-269.
- MACDONALD, E., AND J. HUBERT. 2002. A review of the effects of

- silviculture on timber quality of Sitka spruce. *Forestry* 75(2):107-138.
- MEGRAW, R.A. 1985. Wood quality factors in loblolly pine. The influence of tree age, position in tree, and cultural practice on wood specific gravity, fiber length, and fibril angle. Tappi Press, Atlanta, GA. 88 p.
- MEGRAW, R.A., D. BREMER, G. LEAF, AND J. ROERS. 1999. Stiffness in loblolly pine as a function of ring position and height, and its relationship to microfibril angle and specific gravity. Proceedings of the third workshop—Connection between silviculture and wood quality through modeling approaches. IUFRO S5.01-04:341-349.
- PILLOW, M.Y., B.Z. TERRELL, AND C.H. HILLER. 1953. Patterns of variation in fibril angles in loblolly pine. Mimeo, D1953. USDA Forest Service, Washington, DC. 11 p.
- PINHEIRO, J.C., AND D.M. BATES. 2000. Mixed-effects models in S and S-PLUS. Springer, New York. 528 p.
- WATSON, A.J., AND H.E. DADSWELL. 1964. Influence of fibre morphology on paper properties. 4. Micellar spiral angle. *Appita* 17:151-156.
- WEAR, D.N., AND J.G. GREIS. 2002. Southern forest resource assessment: Summary of findings. *J. For.* 100(7):6-14.
- YING, L., D.E. KRETSCHMANN, AND B.A. BENDTSEN. 1994. Longitudinal shrinkage in fast-grown loblolly pine plantation wood. *Forest Products Journal* 44(1):58-62.